Research Article

Journal of Applied Toxicology

Received: 13 July 2011, Revised: 26 September 2011, Accepted: 20 October 2011 Published online in Wiley Online Library: 7 December 2011

(wileyonlinelibrary.com) DOI 10.1002/jat.1775

Oxidative stress induced by aluminum oxide nanomaterials after acute oral treatment in Wistar rats

P. V. Prabhakar[a], Utkarsh A. Reddy[a], S. P. Singh[a], A. Balasubramanyam[a], M. F. Rahman[a], S. Indu Kumari[a], Sachin B. Agawane[b], U. S. N. Murty[a], Paramjit Grover[a] and Mohammed Mahboob[a]*

ABSTRACT: This study investigated the oxidative stress induced after acute oral treatment with 500, 1000 and 2000 mg kg^{-1} doses of Al_2O_3-30 and −40 nm and bulk Al_2O_3 in Wistar rats. Both the nanomaterials induced significant oxidative stress in a dose-dependent manner in comparison to the bulk. There was no significant difference between the two nanomaterials. However, the effect decreased with increase with time after treatment. The histopathological examination showed lesions only in liver with Al_2O_3 nanomaterials at 2000 mg kg^{-1}. Copyright © 2011 John Wiley & Sons, Ltd.

Keywords: Aluminium oxide nanomaterials; acute oral toxicity; oxidative stress; antioxidant enzymes; histopathology; Wistar rat

INTRODUCTION

Nanomaterials (NMs) are defined as particles designed and produced to have at least one dimension lower than 100 nm. Extensive research involving the use and design of different types of NMs continues to increase the number of nanotechnology applications. This is because of their distinctive properties (e.g. chemical, mechanical, optical, magnetic, and biological), which make them desirable for industrial and healthcare applications (Oberdörster *et al*., 2005). Widespread manufacture and use of nanobased products will generate multiple sources of their release into the environment, water and food supplies, which may result in voluntary or involuntary entry into human body. The characteristic properties of NMs (e. g. high surface area to volume ratio) give them a unique mechanism of toxicity (Aillon *et al*., 2009). For example, the smaller the size of the particle, the deeper it can travel into the organs and slower the clearance rate is from the deposition sites (Wang *et al*., 2009). Moreover, the increased surface area of smaller particles may exhibit greater biological activity, such as an increased generation of reactive oxygen species (ROS) when compared with the usual particles at equivalent mass. Other properties like chemical composition, size and shape may also negate or amplify the surface effects, hence smaller particles are more reactive and have different biological activity from their conventional bulk materials (Oberdörster *et al*., 2005; Nel *et al*., 2006). Both *in vivo* and *in vitro* studies using wide range of NMs have been shown to generate ROS and induction of oxidative stress as one of the appealing mechanisms by which NMs induce adverse effects at the cellular and molecular level (Oberdörster *et al*., 2005; Nel *et al*., 2006; Zhu *et al*., 2008). This is because metallic ions released from metal-derived NMs such as Fe^{2+}, Cu^{+}, Mn^{2+}, Cr^{5+} and Ni^{2+} may contribute to production of ROS via the Fenton-type reaction (Yang *et al*., 2009; Li *et al*., 2010a). Usually cells respond to these ROS by stimulating their antioxidant defense system in order to protect themselves. However, if the defense system fails to neutralize the oxidative burden, the ROS will oxidize cellular proteins, DNA and lipids, and inactivate specific enzymes by oxidation of cofactors, leading to a state called oxidative stress (Kortenkamp *et al*., 1990; Fahmy and Cormier, 2009; Patlolla *et al*., 2011). A large number of studies have demonstrated that NMs have a clear connection with oxidative stress (Zhu *et al*., 2008; Liu *et al*., 2010).

Among various NMs, aluminum oxide (Al_2O_3) NM is one of the most important because of its promising technological applications. It is currently one of the two US market leaders for nano-sized materials (Sadiq *et al*., 2009). Aluminum (Al) and Al_2O_3 NMs are widely used in site-specific drug delivery systems to increase solubility. They are also used in explosives, ammunition, artillery surface coatings, lithium batteries, resistant coatings on propeller shafts, fuels in boosters, missiles and rockets, gelled fuels, the ceramic industry, scratch- and abrasive-resistant coatings on sunglasses, car finishing and flooring, and orthopedic implants (Tyner *et al*., 2004; Monteiro-Riviere *et al*., 2010). Use of nano Al in various applications may lead to release of the oxidized form of nano Al_2O_3 into the environment (Coleman *et al*., 2010). Further, it was reported that Al_2O_3 NMs enhanced the anticancer effects of immunotherapy that employs tumor cell vaccine (Sun *et al*., 2010).

Although Al_2O_3 NMs have a variety of applications, few studies have demonstrated that exposure to nano form of Al_2O_3 may lead to adverse effects, such as genetic damage

*Correspondence to: M. Mahboob, Toxicology Unit, Biology Division, Indian Institute of Chemical Technology, Hyderabad, Andhra Pradesh, India.
Email: mahboobm1983@gmail.com

[a]Toxicology Unit, Indian Institute of Chemical Technology, Hyderabad, Andhra Pradesh, India

[b]Department of Pharmacology, Indian Institue of Chemical Technology, Hyderabad, Andhra Pradesh, India

Journal of Applied Toxicology

(Balasubramanyam *et al*., 2009), inflammatory response (Oesterling *et al*., 2008), carcinogenicity (Dey *et al*., 2008), cytotoxicity (Chen *et al*., 2008; Di Virgilio *et al*., 2010), ROS generation and mitochondrial dysfunction (Chen *et al*., 2008). Nano Al has shown impaired phagocytic function in human alveolar macrophages (Braydich-Stolle *et al*., 2010). Bhalla and Dhawan (2009) and Kumar *et al*. (2009) demonstrated that Al bulk can also induce oxidative stress in rats, but similar literature on nano Al_2O_3 is lacking. Hence, the present study was conducted to compare the oxidative stress-inducing potential of Al_2O_3 NMs and bulk in Wistar rats.

In general, most of the toxic chemicals are metabolized in liver; hence, there is a high risk of free radical attack leading to lipid peroxidation, which in turn leads to hepatotoxicity (Patlolla *et al*., 2011). Kidneys have a very active oxidative metabolism that results in ROS generation, which can damage major cellular components (Mahieu *et al*., 2009). Brain is reported to be especially vulnerable to oxidative stress because of its high metabolic rate and poor antioxidant defense system. The ability of NMs to cross the blood–brain barrier further enhances the risk (Ma *et al*., 2010). Hence, liver, kidneys, heart and brain were selected for studying the oxidative stress-inducing potential of Al_2O_3-30 and −40 nm and the bulk equivalent. Induction of oxidative stress was investigated by assessing reduced glutathione (GSH) as a cellular antioxidant, malondialdehyde (MDA) as a biomarker of lipid peroxidation (LPO), superoxide dismutase (SOD) as it plays an antioxidant role by dismutating superoxide, catalase (CAT) by decomposing hydrogen peroxide, glutathione reductase (GR) by replenishing GSH from oxidized glutathione and glutathione peroxidase (GPx) by detoxifying harmful hydroperoxides, to understand the toxicity mechanism in response to Al_2O_3-30 and −40 nm and the bulk equivalent. The histopathological studies are considered to be an important descriptor for potential toxicity of NMs. Therefore another aim of this study was to evaluate the histopathological changes in various tissues treated with Al_2O_3-30 and −40 nm and the bulk equivalent.

MATERIALS AND METHODS

Materials

Al_2O_3-30 nm and Al_2O_3-40 nm (product codes M1056 and M1049-D) were gifts from Dr Karl Martin of Nova Centrix, USA (purity >90%), Al_2O_3-bulk was purchased from Sigma Aldrich Inc., purity 90%. *n*-Butanol, nicotinamide adenine dinucleotide phosphate (*β*-NADPH), pyrogallol and glutathione reductase were purchased from Sigma Aldrich Inc. Ethylenediamine tetraacetic acid disodium salt (Na_2EDTA), trichloroacetic acid (TCA), 2-thiobarbituric acid (TBA), 5-sulfosalicylic acid, sodium citrate, hydrogen peroxide, 5,5-dithiobis-2-nitrobenzoic acid (DTNB), 1-chloro-2,4-dinitrobenzene (CDNB), GSH, hydrogen peroxide (H_2O_2) and hydrochloric acid (HCl) were purchased from Himedia Laboratories, India.

Animals

Healthy adult female albino Wistar rats of 8–10 week old were purchased from the National Institute of Nutrition, Hyderabad, India. Animals were maintained under standard laboratory conditions, including temperature 22 ± 2 °C, relative humidity 50–60% and constant 12 h light–dark cycle. The animals were fed on commercial pellet diet and water *ad libitum*. Animals were allowed to acclimatize to laboratory conditions for 7 days prior to the start of experiments. All procedures were reviewed and approved by Institutional Animal Ethics Committee of our organization.

Treatment

The animals were randomly selected, marked and kept in separate cages before commencement of the study. The rats were fasted overnight prior to dosing. Animals were divided into 10 groups (10 rats per group): the control group and nine experimental groups. The NMs were suspended in 1% Tween-80. Experimental groups were treated with Al_2O_3-30 nm, Al_2O_3-40 nm and Al_2O_3-bulk by single oral doses of 500, 1000 and 2000 mg kg^{-1}. The control group was treated with an equal volume of 1% Tween-80. These doses were drawn from our previous acute oral toxicity study of Al_2O_3-30 nm, -40 nm and -bulk in Wistar rats (Balasubramanyam *et al*. 2009). After the treatment the test animals were observed for symptoms and mortality every day for 14 days. On days 3 and 14, five animals from each group were sacrificed after being anesthetized with pentothal and isofluorane. Liver, kidneys, brain and heart tissues were collected from each animal, rinsed in ice cold physiological saline, perfused with cold potassium chloride buffer (1.15% KCl and 0.5 mM EDTA) and homogenized in potassium phosphate buffer (KPB, 0.1 M, pH 7.4). MDA levels and GSH content were measured at this stage. The homogenate was then centrifuged at 15 000 rpm for 30 min to remove debris. The clear supernatant was collected and stored as aliquots in −85 °C until antioxidant enzyme assay. A part of each tissue was stored in 10% formalin for histopathological study.

Lipid Peroxidation

Malondialdehyde, a lipid peroxidation end product in tissue homogenate, was measured according to the method described by Wills (1969) with some modifications. A 200 μL aliquot of tissue homogenate was mixed with 2 ml of thiobarbituric acid (TBA)–trichloroacetic acid (TCA) reagent (0.375 and 15%, respectively). The volume was made up to 3 ml with distilled water and boiled on a water bath at 95 °C for 20 min. The solution was then cooled under tap water. The reaction product (TBA–MDA complex) was extracted by adding 3 ml of *n*-butanol to the above solution. The absorbance of the pink colored extract in *n*-butanol was measured at 532 nm using a spectrophotometer (Spectramax Plus, Molecular Devices, USA). The amount of MDA was calculated using a molar extinction coefficient of $1.56 \times 10^5\ M^{-1}\ cm^{-1}$ and expressed as nmoles of MDA formed per gram wet weight of tissue.

Reduced Glutathione

The reduced glutathione content was measured using the method of Jollow *et al*. (1974). An aliquot of 0.5 ml of each tissue homogenate was incubated with 0.5 ml of sulfosalicylic acid (4% w/v) for 1 h in ice and centrifuged at 10 000 rpm for 10 min. A 0.4 ml aliquot of the supernatant was mixed with 0.4 ml of DTNB (4 mg ml^{-1} in 5% sodium citrate) and 2.2 ml KPB (0.1 M, pH 7.4). The yellow color developed was read at 412 nm. The amount of GSH present was expressed as micrograms GSH per gram wet weight of tissue.

Assay of Antioxidant Enzyme Activities

Superoxide dismutase. Superoxide dismutase activity was estimated in tissue supernatant using the method of Marklund and Marklund (1974). A 3 ml aliquot of assay mixture contained 50 mM Tris–HCl buffer (pH 8.2) with 1 mM diethylene triamine penta acetic acid, 45 µl of 10 mM pyrogallol in 10 mM HCl and 10 µl of tissue supernatant. The rate of inhibition of pyrogallol auto-oxidation after the addition of enzyme extract was noted at 420 nm. The amount of enzyme required to give 50% inhibition of pyrogallol auto-oxidation was considered as one unit of enzyme activity. The enzyme activity was expressed as units per milligram protein. The protein content in the tissue supernatant was estimated using standard protocol (Lowry *et al.* 1951). Bovine serum albumin was used as standard.

Catalase. The catalase activity was assayed spectrophotometrically using the method of Aebi (1984). Briefly, the assay mixture of 3 ml contained 0.063% H_2O_2 in 0.1 M KPB pH 7.4 and 10 µl of tissue supernatant. The decrease in absorbance was recorded for 1 min at 240 nm. The enzyme activity was expressed as mmol of H_2O_2 decomposed per minute per milligram protein using a molar extinction coefficient of 43.6 $M^{-1}\,cm^{-1}$. The activity was expressed as units per milligram protein.

Glutathione peroxidase. The glutathione peroxidase activity was measured using the procedure of Paglia and Valentine (1967). The enzyme assay was performed by adding 750 µl of KPB (0.1 M, pH 7), 60 µl NADPH (2.25 mM in 0.1% $NaHCO_3$), 15 µl of glutathione reductase (7.1 µl ml^{-1}) and 25 µl GSH (11.52 mg ml^{-1}) in a 1 ml cuvette. The enzymatic reaction was initiated by adding 50 µl supernatant and 100 µl of hydrogen peroxide (1.5 mM). The decrease in absorbance at 340 nm was observed for 1 min in the spectrophotometer. The enzyme activity was expressed as micromoles of NADPH oxidized per minute using molar extinction coefficient of $6.22 \times 10^3\,mmol^{-1}\,cm^{-1}$. The GPx activity was expressed in units/mg protein.

Glutathione reductase. The glutathione reductase activity was assayed using the method of Carlberg and Mannervik (1985). In a 3 ml reaction mixture, 50 mM KPB, 1.0 mM oxidized glutathione, 0.15 mM β- NADPH and 0.01% (w/v) bovine serum albumin were taken and 20 µl of tissue supernatant was added. The reaction mixture was immediately mixed by inversion and the decrease in the absorbance was recorded at 340 nm. The enzyme activity was expressed as micromoles β-NADPH decomposed per minute per milligram protein using a molar extinction coefficient of $6.22 \times 10^3\,mmol^{-1}\,cm^{-1}$. The GR activity was expressed in units per milligram protein.

Glutathione S-transferase. The GST activity was determined according to the method of Habig *et al.* (1974). The reaction mixture consisted of 2.75 ml KPB (0.1 M, pH 6.5), 0.1 ml GSH (75 mM), 0.1 ml CDNB (30 mM in 95% ethanol) and 0.05 ml supernatant in a total volume of 3 ml in a cuvette. The change in absorbance was recorded at 340 nm for 2 min. The enzyme activity was expressed as µmol CDNB-conjugate per minute per millgram protein using a molar extinction coefficient of $9.6 \times 10^3\,M^{-1}\,cm^{-1}$. The GST activity was expressed in units per milligram protein.

Histopathological Examination

The animals were sacrificed on day 14 after a single oral treatment of Al_2O_3-30 nm, -40 nm, or -bulk and examined for gross lesions. Part of each of the liver, kidneys, heart and brain was fixed in 10% formalin for preparation of histological slides. The tissues were processed in a Leica TP 1020 tissue processor, then embedded in paraffin blocks using Leica EG 1160 paraffin embedder. The paraffin blocks were cut into ribbons of 4 µm using a Microm HM 360 microtome. The slides were stained in hemotoxylin and eosin using a Microm HMS-70 stainer. The permanent slides were made and evaluated for histopathological changes under Olympus BX51 microscope. The slides were coded to avoid possible bias before analysis.

Table 1. Acute effect of aluminum oxide nanomaterials and bulk on MDA levels (nanomoles of MDA per gram wet tissue) in various tissues of rat on days 3 and 14

Tissue	Dose (mg kg^{-1})	Day 3				Day 14		
		Control	30 nm	40 nm	Bulk	30 nm	40 nm	Bulk
Liver	2000	10.5 ± 1.6	33.6 ± 5.3***[a]	29.8 ± 4.3***[a]	15.0 ± 1.3	14.8 ± 2.1*	13.6 ± 1.1	12.36 ± 1.1
	1000	10.5 ± 1.6	23.4 ± 4.9*[a]	24.1 ± 6.0*[a]	13.2 ± 0.3	10.8 ± 1.8	10.7 ± 1.2	10.97 ± 1.1
	500	10.5 ± 1.6	14.5 ± 0.9**[a]	13.7 ± 0.6*[a]	10.8 ± 0.7	10.6 ± 1.0	9.33 ± 0.9	10.25 ± 1.1
Kidneys	2000	8.39 ± 1.2	13.4 ± 1.5**	12.2 ± 0.9*	11.7 ± 1.2*	7.2 ± 0.9	7.7 ± 0.7	7.9 ± 0.6
	1000	8.39 ± 1.2	9.95 ± 0.5	8.93 ± 0.6	7.96 ± 0.15	9.0 ± 0.9	8.6 ± 0.8	9.5 ± 0.6
	500	8.39 ± 1.2	8.73 ± 0.7	8.51 ± 0.7	8.27 ± 0.9	8.0 ± 0.8	8.4 ± 0.6	8.5 ± 0.8
Brain	2000	12.3 ± 1.1	16.7 ± 1.7*[a]	14.4 ± 1.4	12.5 ± 1.3	12.3 ± 1.1	11.6 ± 1.4	11.6 ± 1.2
	1000	12.3 ± 1.1	13.1 ± 1.0	12.7 ± 1.2	12.2 ± 1.2	12.0 ± 1.3	11.6 ± 1.2	12.1 ± 1.4
	500	12.3 ± 1.1	13.2 ± 1.2	11.0 ± 1.5	12.8 ± 1.1	11.6 ± 1.0	12.0 ± 0.7	11.4 ± 1.3
Heart	2000	2.84 ± 0.6	2.8 ± 0.3	2.43 ± 0.9	2.5 ± 0.8	2.8 ± 0.7	2.4 ± 0.9	2.56 ± 0.87
	1000	2.84 ± 0.6	2.2 ± 0.8	2.14 ± 0.9	2.2 ± 0.7	2.8 ± 0.5	2.6 ± 0.9	2.26 ± 0.63
	500	2.84 ± 0.6	2.8 ± 0.5	2.38 ± 0.8	3.0 ± 0.9	2.6 ± 0.7	2.7 ± 0.7	3.09 ± 0.62

Each value represents the mean ± SD; $n = 5$ rats.
*** $P < 0.001$; ** $P < 0.01$; * $P < 0.05$ when compared with controls.
[a] $P < 0.05$ when compared with bulk.
MDA, Malondialdehyde.

Journal of Applied Toxicology

Table 2. Acute effects of aluminum oxide nanomaterials and bulk on reduced GSH content (micrograms GSH per gram wet tissue) in various tissues of rat on days 3 and 14

Tissue	Dose (mg kg^{-1})	Day 3				Day 14		
		Control	30 nm	40 nm	Bulk	30 nm	40 nm	Bulk
Liver	2000	592.5 ± 20.2	427.1 ± 26.5***[a]	422.6 ± 33.9***[a]	494.1 ± 14.1**	519.6 ± 23.6	524.3 ± 36.9	520.3 ± 29.9
	1000	592.5 ± 20.2	439.6 ± 34.5***	478.4 ± 23.8**	501.7 ± 17.3**	565.5 ± 36.2	564.1 ± 20.2	575.8 ± 34.0
	500	592.5 ± 20.2	506.0 ± 29.0**	507.2 ± 25.2**	520.2 ± 18.5*	591.9 ± 28.5	593.4 ± 15.2	586.9 ± 26.9
Kidneys	2000	409.5 ± 30.6	310.9 ± 27.5*	306.4 ± 29.3*	307.1 ± 30.2*	381.2 ± 19.4	388.9 ± 26.9	382.2 ± 15.4
	1000	409.5 ± 30.6	318.0 ± 19.7**	324.0 ± 14.4**	327.4 ± 25.2*	395.2 ± 32.2	383.4 ± 31.8	379.9 ± 33.5
	500	409.5 ± 30.6	352.4 ± 18.1*	355.0 ± 6.69	346.9 ± 21.6*	409 ± 27.5	406.3 ± 22.0	404.0 ± 22.9
Brain	2000	248.5 ± 36.7	138.2 ± 21.4**	145.9 ± 22.3**	154.4 ± 25.1*	241.0 ± 30.7	225.9 ± 21.2	232.8 ± 26.7
	1000	248.5 ± 36.7	169.3 ± 17.6*	168.7 ± 24.1*	169.9 ± 17.9*	233.2 ± 21.9	249.9 ± 37.7	249.6 ± 15.4
	500	248.5 ± 36.7	187.6 ± 4.27*	182.6 ± 13.8*	186.4 ± 8.12*	265.4 ± 7.4	248.7 ± 16.9	236.0 ± 34.2
Heart	2000	85.2 ± 9.3	84.1 ± 7.4	84.5 ± 9.3	84.5 ± 4.7	89.6 ± 8	85.7 ± 7.5	82.8 ± 5.6
	1000	85.2 ± 9.3	82.3 ± 8.7	88.2 ± 9.5	84.9 ± 8.0	88.9 ± 6.5	74.9 ± 6.9	82.6 ± 9.9
	500	85.2 ± 9.3	83.5 ± 5.8	85.6 ± 7.7	83.6 ± 8.7	83.6 ± 6.9	81.0 ± 2.6	73.6 ± 5.5

Each value represents the mean ± SD; $n = 5$ rats.
*** $P < 0.001$; ** $P < 0.01$; * $P < 0.05$ when compared with controls.
[a] $P < 0.05$ when compared with bulk.
GSH, Reduced glutathione.

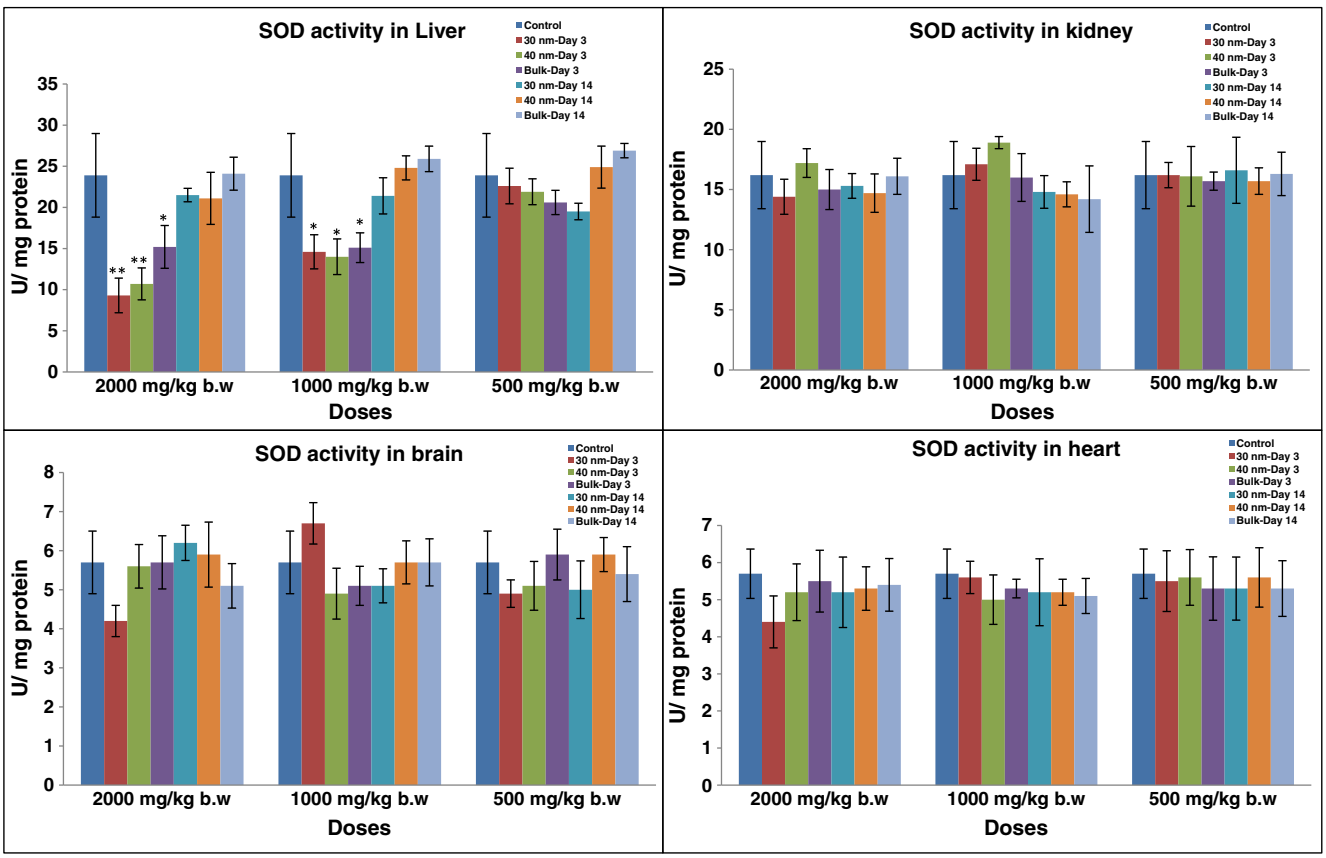

Figure 1. Acute effects of Al_2O_3 nanomaterials and bulk on superoxide dismutase activity in various tissues of rat on days 3 and 14. Each value represents the mean ± SD; $n = 5$ rats. *** $P < 0.001$; ** $P < 0.01$; * $P < 0.05$ when compared with controls.

Statistical Analysis

All the data was expressed as means ± standard deviation (SD). The means and standard deviations were calculated according to the standard methods for all the parameters. The *P*-values were calculated in GraphPad InStat by one-way ANOVA followed by a Turkey–Kramer multiple comparison test by comparing different groups (control group vs treatment groups and bulk vs nanomaterial groups). The value of $P < 0.05$ was considered to be statistically significant.

RESULTS

Body Weight, Feed Intake, Organ Weights and Clinical Signs

The acute oral treatment of Al_2O_3 NMs and bulk caused no significant change in body weight gain, feed intake and organ weights of treated rats when compared with controls. Clinical signs and symptoms were not observed in the treated rats (data not shown).

Lipid Peroxidation

Lipid peroxidation assay was performed to determine the MDA levels in tissue homogenate of Al_2O_3-30 nm, -40 nm and -bulk-treated rats and the results are presented in Table 1. On day 3, the MDA levels of liver were significantly increased in Al_2O_3-30 and −40 nm-treated rats in all the dose groups in a dose-dependent manner when compared with control and bulk groups. Similarly, significantly elevated MDA levels were observed in kidneys of Al_2O_3-30 nm, -40 nm and -bulk-treated rats at 2000 mg kg^{-1}. However, in brain Al_2O_3-30 nm at 2000 mg kg^{-1} dose showed significantly higher MDA levels when compared with controls as well as the bulk group. On day 14 only liver showed significantly increased MDA levels in Al_2O_3-30 nm-treated rats at 2000 mg kg^{-1}. The heart tissue did not show significant change in MDA levels at both the time intervals. We observed no significant difference in MDA levels between 30 and 40 nm-treated groups, but when compared with the bulk group, NM treated rats showed significantly enhanced MDA levels, suggesting that these NMs were more potent in inducing oxidative stress via the lipid peroxidation process.

Reduced Glutathione Content

Table 2 summarizes the changes in reduced glutathione content in different tissues of rats following acute oral treatment with Al_2O_3-30 nm, -40 nm and -bulk. On day 3, Al_2O_3-30 nm, -40 nm and -bulk treatment caused a significant dose-dependent decrease in GSH levels in liver, kidneys and brain when compared with controls. Only Al_2O_3-30 and −40 nm treatment at 2000 mg kg^{-1} dose showed significant decrease in GSH content from treatment with Al_2O_3-bulk. On day 14, Al_2O_3-30 nm, -40 nm and -bulk-treated groups showed normal levels of GSH in all the tissues. Heart tissue did not show any change in glutathione content. Furthermore, Al_2O_3-NM treatment caused greater depletion in GSH content than the bulk.

Superoxide Dismutase Activity

The effect of Al_2O_3-30 nm, -40 nm and -bulk on SOD activity is presented in Fig. 1. On day 3, Al_2O_3-30 nm, -40 nm and -bulk treatment at 1000 and 2000 mg kg^{-1} caused significant inhibition in the SOD activity of liver. However, kidneys, brain and heart tissues showed no significant change in SOD activity. On day 14, no significant alteration in SOD activity was found in Al_2O_3-30 nm, -40 nm and -bulk-treated rats. The NM treatment caused more inhibition in SOD activity than bulk.

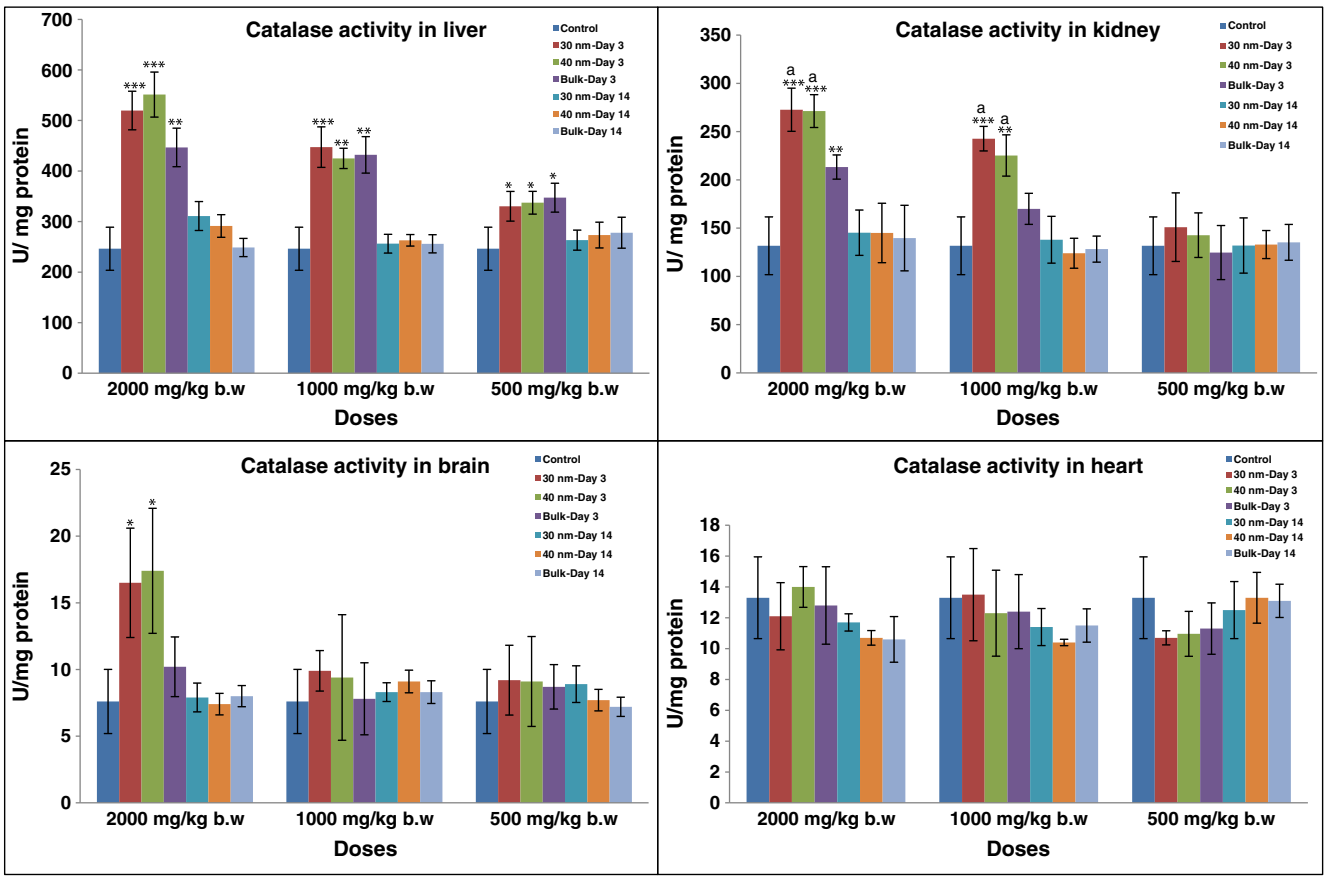

Figure 2. Acute effects of Al_2O_3 nanomaterials and bulk on catalase activity in various tissues of rat on days 3 and 14. Each value represents the mean ± SD; $n = 5$ rats. *** $P < 0.001$; ** $P < 0.01$; * $P < 0.05$ when compared with controls. [a] $P < 0.05$ when compared with bulk.

Catalase Activity

Figure 2 summarizes the changes in CAT activity in liver, kidneys, heart and brain tissues. On day 3, the Al_2O_3-30 nm, -40 nm and -bulk-treated rats showed significant increase in CAT activity in liver at 500, 1000 and 2000 mg kg^{-1} doses in a dose-dependent manner. In kidneys, Al_2O_3-30 and −40 nm treatment at 1000 and 2000 mg kg^{-1} significantly enhanced CAT activity in a dose-dependent manner when compared with controls and bulk. In brain, Al_2O_3-30 and −40 nm-treated rats showed significant increase in CAT activity at 2000 mg kg^{-1}. On day 14, significant differences was not observed in CAT activity at any dose of Al_2O_3-30 nm, -40 nm and -bulk. The increase in CAT activity with Al_2O_3 NMs was higher than that with bulk material.

Glutathione Peroxidase Activity

The acute oral treatment of Al_2O_3-30 nm, -40 nm and -bulk caused no significant change in GPx activity in all the tissues at any dose levels (data not shown).

Glutathione Reductase Activity

The GR activity in Al_2O_3-30 nm, -40 nm and -bulk-treated and control rats is presented in Fig. 3. On day 3, in liver, Al_2O_3-30 and −40 nm at 500, 1000 and 2000 mg kg^{-1} and Al_2O_3-bulk at 1000 and 2000 mg kg^{-1} treatment resulted in a significant dose-dependent decrease in glutathione reductase activity when compared with controls. However, in kidneys from rats treated with Al_2O_3-30 and −40 nm at 1000 and 2000 mg kg^{-1} and bulk at 2000 mg kg^{-1} showed significantly decreased glutathione reductase activity. Brain and heart tissues showed normal levels of GR activity after treatment with Al_2O_3-30 nm, -40 nm and -bulk when compared with controls. On day 14, Al_2O_3-30 nm, -40 nm and -bulk treatment did not cause significant change in GR activity. Further, the inhibition in GR activity by nano Al_2O_3 was higher than its bulk.

Glutathione *S*-transferase Activity

The acute effects on GST activity in different tissues of treated and control rats are presented in Fig. 4. On day 3, Al_2O_3-30 and −40 nm-treated rats showed significant increase in GST activity in liver (500, 1000 and 2000 mg kg^{-1}), kidneys (2000 mg kg^{-1}) and brain (2000 mg kg^{-1}) in a dose-dependent manner. Al_2O_3-bulk treatment enhanced GST activity in liver at 1000 and 2000 mg kg^{-1}, and in kidneys at 2000 mg kg^{-1}. On day 14, GST activity in all the treated groups recovered to normal as controls. The results revealed that the nano-Al_2O_3 treatment induced GST activity more significantly than the bulk.

Histopathology

The histopathological changes in brain, liver, kidneys and heart studied on day 14 day after acute oral treatment of

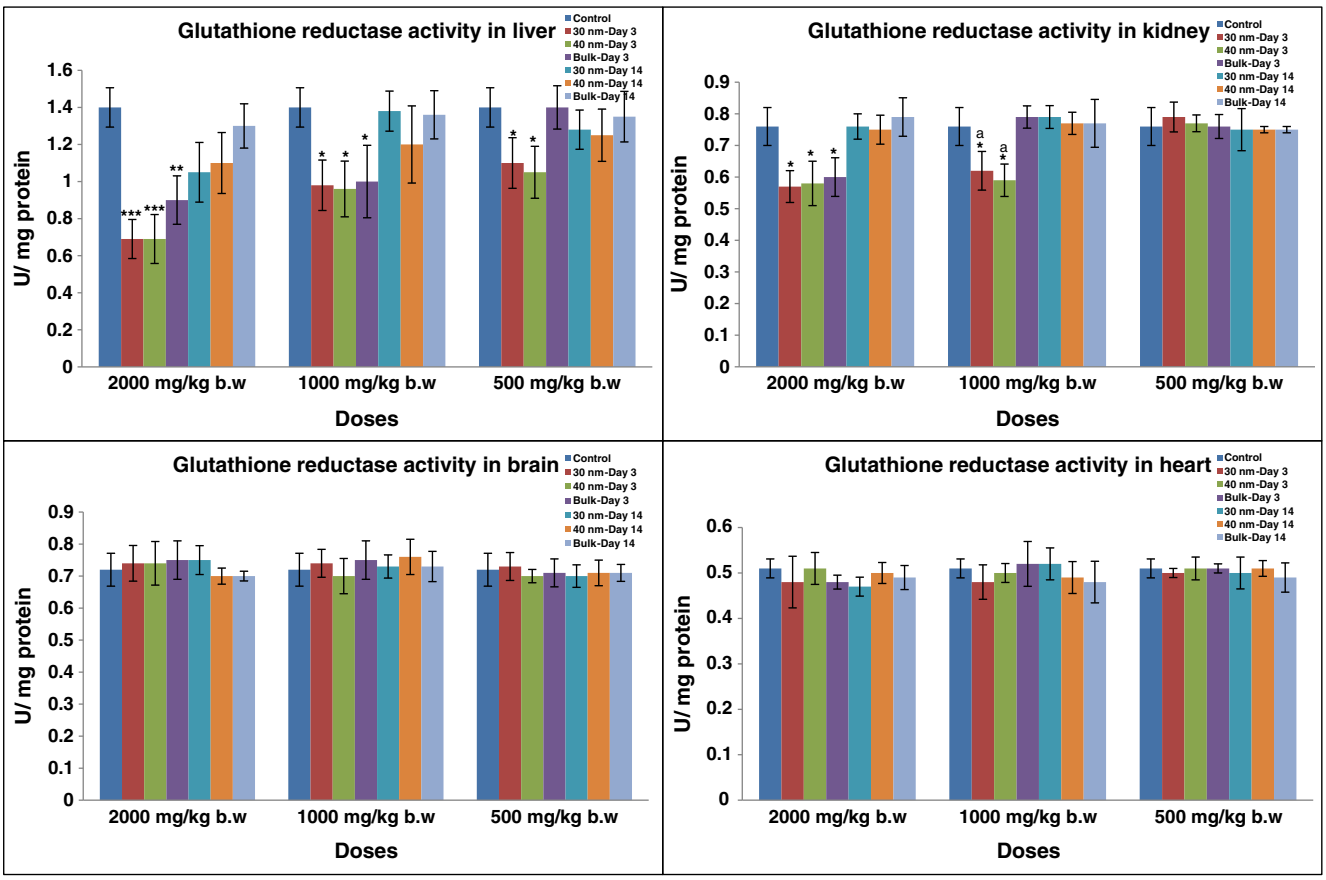

Figure 3. Acute effects of Al_2O_3 nanomaterials and bulk on glutathione reductase activity in various tissues of rat on days 3 and 14. Each value represents the mean ± SD; $n = 5$ rats. *** $P < 0.001$; ** $P < 0.01$; * $P < 0.05$ when compared with controls. [a] $P < 0.05$ when compared with bulk.

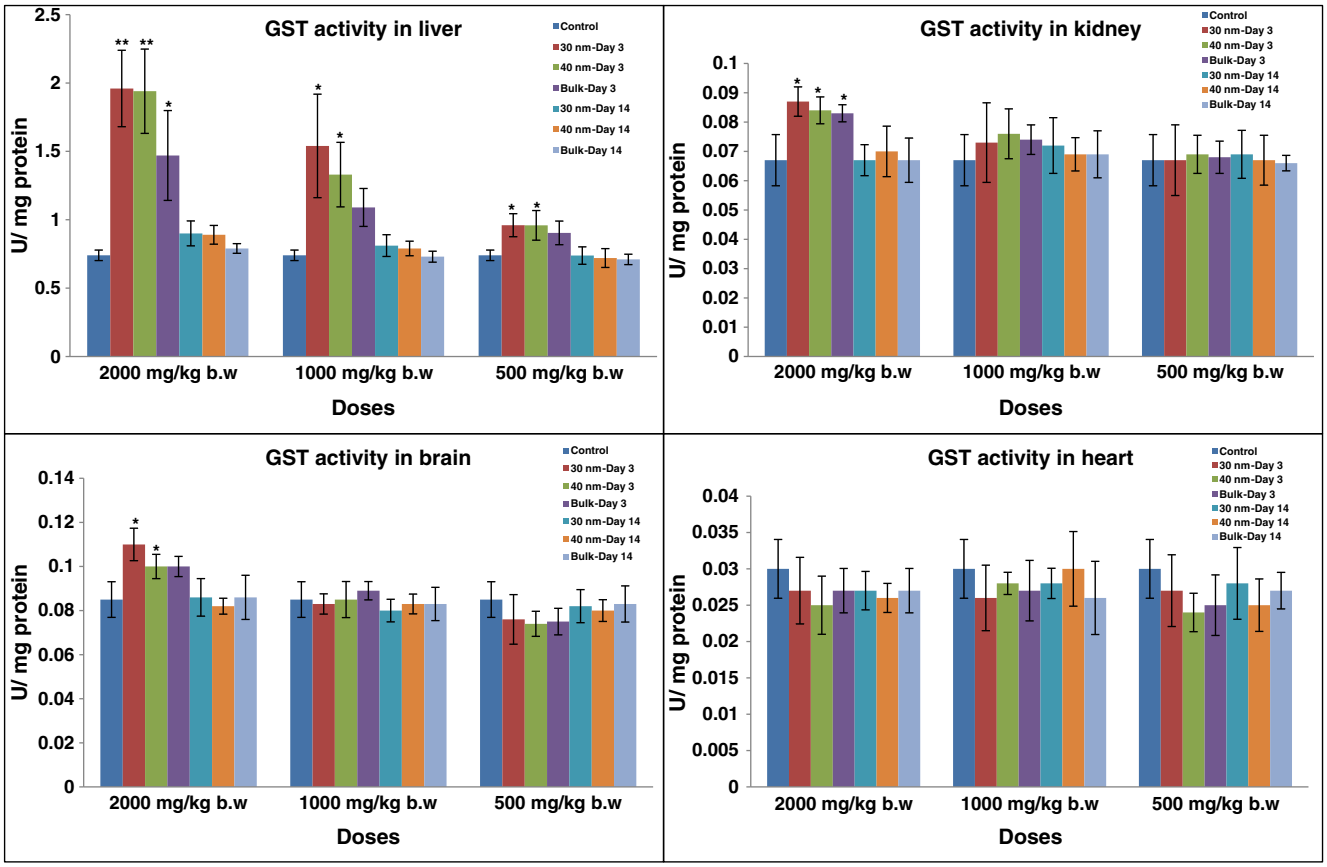

Figure 4. Acute effects of Al_2O_3 nanomaterials and bulk on glutathione *S*-transferase activity in various tissues of rat on days 3 and 14. Each value represents the mean ± SD; $n = 5$ rats. *** $P < 0.001$; ** $P < 0.01$; * $P < 0.05$ when compared with controls.

Al_2O_3-30 nm, -40 nm and -bulk are presented in Fig. 5. In 500 and 1000 mg kg^{-1} dose groups of Al_2O_3-30 and −40 nm, the tissues showed no abnormal pathological changes when compared with the control. In the 2000 mg kg^{-1} dose group of Al_2O_3-30 and −40 nm, significant histopathological changes were observed only in the liver tissue, i.e. dilated central veins and expanded portal tracts. These pathological changes were observed in 30% of all the experimental animals examined. Al_2O_3-bulk treatment at all the dose levels revealed normal histology.

DISCUSSION

In the current investigation, two different sizes of NMs along with bulk material were used. Since the manufacturer had mentioned Al_2O_3-30 and −40 nm as two different sizes, our concern was to know whether this 10 nm difference in the two NMs was sufficient to produce variations in oxidative stress. When we consider the sizes at nanoscale, the 10 nm variation between two different sizes may correspond to discrete toxic effects. Therefore, we treated them as two different groups to ascertain the potential oxidative stress effects *in vivo*. Similarly, Wagner *et al.* (2007) and Murdock *et al.* (2008) also regarded Al_2O_3-30 nm and −40 nm as two different treatment groups to study the toxic effects on mammalian cell lines.

In this study, we have attempted to determine the role of oxidative stress as a critical factor in Al_2O_3 NM-induced toxicity in treated rats, since oxidative stress is considered to be an important mechanism in carcinogenesis (De Berardis *et al.*, 2010). The present study demonstrated that the MDA levels were significantly elevated in Al_2O_3-30 and −40 nm-treated groups in a dose-dependent mode, suggesting that NMs might have induced free radical generation that further initiated LPO. The GSH levels were decreased after Al_2O_3-NM and -bulk treatment in a dose-dependent manner, possibly owing to increased utilization of GSH in neutralizing free radicals generated. When excessive ROS are produced, the levels of LPO will rise and GSH levels will decline, signifying that the treated rats suffered severe oxidative stress condition.

The endogenous antioxidant system comprising SOD, CAT, GPx and GR plays important roles in free radical and peroxide metabolism and is responsible in part for protecting the cells against oxidant stress (Wang *et al.*, 2006). In this study we observed that the increase in LPO and depletion in GSH content were accompanied by a dose-dependent increase in CAT activity, and a decrease in SOD and GR activities with no change in GPx activity after acute oral treatment with Al_2O_3 NMs and bulk. In antioxidant enzymes, SOD is always considered as the first line of defense against oxygen toxicity owing to its inhibitory effects on oxy radical formation (Li *et al.*, 2010b). In this study, the increase in dose of Al_2O_3 NMs and bulk strongly inhibited the SOD activity. This inhibition in SOD activity could be due to the high flux of superoxide radicals resulting in H_2O_2 production in cells (Li *et al.*, 2010b). The H_2O_2 in cells is further responsible for the changes observed in the activities of antioxidant

Journal of AppliedToxicology

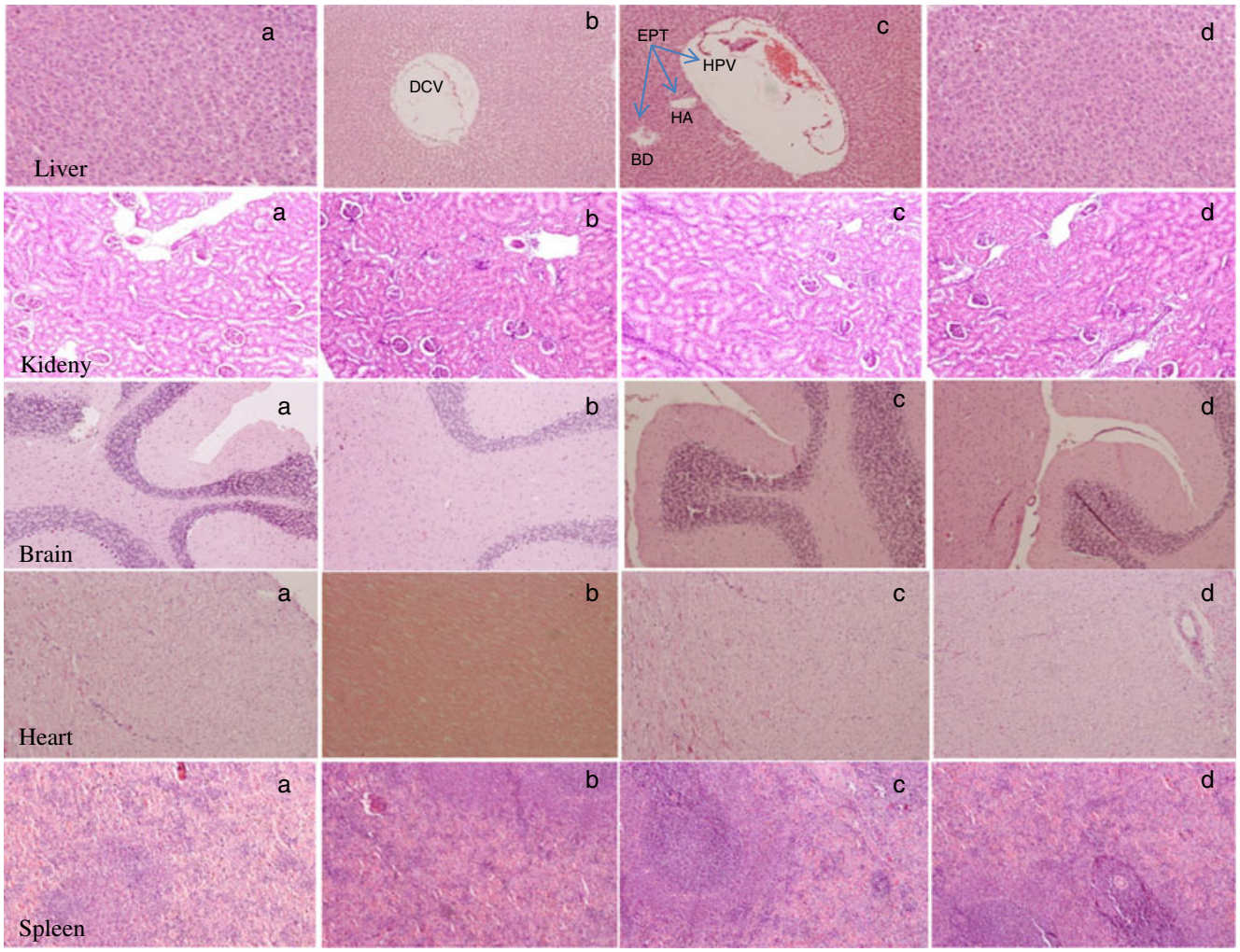

Figure 5. Photomicrographs of the liver, kidneys, brain (cerebellum), heart (ventricular wall) and spleen from (a) the control, and (b) Al_2O_3-30 nm-, (c) Al_2O_3-40 nm- and (d) Al_2O_3-bulk-treated rats at 2000 mg kg^{-1} on day 14 post oral administration. Observation was made at 40× magnification. DCV, Dilated central vein; EPT, expanded portal tract, including hepatic artery (HA), hepatic portal vein (HPV) and bile duct (BD).

enzymes in this study. Particularly high levels of H_2O_2 up-regulate CAT activity and down-regulate the activity of SOD (Fernández-Urrusuno *et al*., 1997). CAT is extensively involved in the degradation of resulting H_2O_2. GPx also catalyzes the reduction of H_2O_2 and lipid peroxides at the expense of GSH. Although CAT and GPx share the same substrate, i.e. H_2O_2, but with different affinities, GPx is more effective at low levels of H_2O_2 and CAT is more effective at high levels of H_2O_2. The decreased SOD activity, increased CAT activity and no change in GPx activity in our study suggest that Al_2O_3-NM and bulk treatment resulted in high levels of H_2O_2 production (Fernández-Urrusuno *et al*., 1997; Powers and Jackson 2008). Al_2O_3-NM and -bulk exposure depleted the activity of GR, probably owing to deficient production of oxidized glutathione back from GSH mediated by GPx (Li *et al*., 2010b). GST metabolizes a variety of carcinogens by conjugating lipophilic electrophiles to GSH. In Al_2O_3 NM- and bulk-treated rats, GST activity was elevated in liver, kidneys and brain. Increased participation of GSH in conjugation reactions mediated by increased GST activity and decreased glutathione reductase activity, which functions in the regeneration of cellular GSH, may also explain the decrease in the level of GSH after Al_2O_3-NM and -bulk treatment. The alterations in enzymatic antioxidants were dose- and time-dependent and reached normal levels, suggesting the reversal of the effects caused by the NMs after 14 days after treatment. Pathological studies revealed that the liver of Al_2O_3-30 and −40 nm-treated groups showed significant pathological changes, i.e. dilated central veins along with expanded portal tracts.

The results obtained with oxidative stress parameters are in line with Transmission Electron Microscopy (TEM) and Dynamic Light Scattering (DLS) data observed in our previous study, where the mean values of Al_2O_3-30 and −40 nm (as specified by the manufacturer) using TEM were 39.9 ± 31.3 and 47.3 ± 36.1 nm (mean ± SD), respectively. There was no significant difference between the two mean sizes. The DLS measurements of Al_2O_3-30 and −40 nm dispersed in 1% Tween 80 were 138.8 and 147.3 nm, respectively, which were also not significantly different. Likewise, biodistribution of Al content showed that both of the NMs accumulated significantly more than the bulk (Balasubramanyam *et al*., 2009). This is the probable reason for observed insignificant differences between two NMs in oxidative stress and simultaneous significantly higher oxidative stress of NMs when compared with the bulk.

Our data is also in accordance with several other *in vivo* and *in vitro* studies using different NMs that have reported the ability of NMs to induce oxidative stress. Titanium dioxide (TiO_2) NM injected in the abdominal cavity of mice for 14 days significantly increased LPO, decreased GSH levels and altered antioxidant enzyme activity in a dose-dependent manner along with histopathological changes in brain which were more severe when compared with TiO_2 bulk (Ma *et al*., 2010). Similarly, an *in vitro* study on primary mouse embryo fibroblast cells treated with carbon nanotubes, carbon black, silicon dioxide and zinc oxide increased LPO, and depleted GSH content and SOD activity in a dose-dependent manner (Yang *et al*., 2009). Zhu *et al*. (2008) showed that nano and submicron-sized Fe_2O_3 intratracheal instillation produced oxidative stress whereas nano-Fe_2O_3 increased cell lysis in lung epithelium and affected blood coagulation parameters more significantly than submicron-sized Fe_2O_3. Our Al_2O_3-bulk results are also in agreement with Al-bulk administered in the form of $AlCl_3$ through oral gavage, which showed significant induction in LPO in both the cerebrum and cerebellum as compared with normal controls (Bhalla and Dhawan, 2009). Chen *et al*. (2006) showed dose-dependent pathological changes in Imprinting Control Region (ICR) mice after acute oral treatment with nano-copper in kidneys, spleen and liver and no pathological changes in mice treated with micro-copper.

The purpose of the present study was to evaluate the oral toxicity of nanoscale Al_2O_3 in rats according to OECD (2001) guidelines. Hence, the doses used in this investigation were higher than the possible exposure levels. From the present study it was also observed that Al_2O_3-NM toxicity was mainly mediated through the altered antioxidant status of the cells. The present findings will add to the increasing body of evidence that exposure to Al_2O_3 NMs may lead to harmful biological responses. Therefore, further toxicological studies are required to evaluate the hazards of occupational or environmental exposure to NMs.

Acknowledgments

We thank the Department of Biotechnology (DBT), New Delhi for financial support. We are also grateful to DBT, New Delhi for providing fellowships to P.V.P., U.T.K. and S.P.S. The authors express their sincere thanks to Dr J. S. Yadav, Director, Indian Institute of Chemical Technology, Hyderabad for providing facilities and his encouragement during the study.

REFERENCES

Aebi H. 1984. Catalase. In Methods in Enzymology, vol. **105**, Packer L (ed). Academic Press: Orlando, FL; 121–126.

Aillon KL, Xie Y, El-Gendy N, Berkland CJ, Forrest ML. 2009. Effects of nanomaterial physicochemical properties on in vivo toxicity. *Adv. Drug Deliv. Rev.* **61**: 457–466.

Balasubramanyam A, Sailaja N, Mahboob M, Rahman MF, Hussain SM, Grover P. 2009. *In vivo* genotoxicity assessment of aluminium oxide nanomaterials in rat peripheral blood cells using the comet assay and micronucleus test. *Mutagenesis* **24**: 245–251.

Bhalla P, Dhawan DK. 2009. Protective role of lithium in ameliorating the aluminium-induced oxidative stress and histological changes in rat brain. *Cell. Mol. Neurobiol.* **29**: 513–521.

Braydich-Stolle LK, Speshock JL, Castle A, Smith M, Murdock RC, Hussain SM. 2010. Nanosized aluminum altered immune function. *ACS Nano* **4**: 3661–3670.

Carlberg I, Mannervik B. 1985. Glutathione reductase. *Meth. Enzymol.* **113**: 484–490.

Chen L, Yokel RA, Hennig B, Toborek M. 2008. Manufactured aluminum oxide nanoparticles decrease expression of tight junction proteins in brain vasculature. *J. Neuroimmune Pharmacol.* **3**: 286–295.

Chen Z, Meng H, Xing G, Chen C, Zhao Y, Jia G, Wang T, Yuan H, Ye C, Zhao F, Chai Z, Zhu C, Fang X, Ma B, Wan L. 2006. Acute toxicological effects of copper nanoparticles *in vivo*. *Toxicol. Lett.* **163**: 109–120.

Coleman JG, Johnson DR, Stanley JK, Bednar AJ, Weiss CA Jr, Boyd RE, Steevens JA. 2010. Assessing the fate and effects of nano aluminum oxide in the terrestrial earthworm, *Eisenia fetida*. *Environ. Toxicol. Chem.* **29**: 1575–1580.

De Berardis B, Civitelli G, Condello M, Lista P, Pozzi R, Arancia G, Meschini S. 2010. Exposure to ZnO nanoparticles induces oxidative stress and cytotoxicity in human colon carcinoma cells. *Toxicol. Appl. Pharmacol.* **246**: 116–127.

Dey S, Bakthavatchalu V, Tseng MT, Wu P, Florence RL, Grulke EA, Yokel RA, Dhar SK, Yang HS, Chen Y, St Clair DK. 2008. Interactions between SIRT1 and AP-1 reveal a mechanistic insight into the growth promoting properties of alumina (Al_2O_3) nanoparticles in mouse skin epithelial cells. *Carcinogenesis* **29**: 1920–1929.

Di Virgilio AL, Reigosa M, de Mele MF. 2010. Response of UMR 106 cells exposed to titanium oxide and aluminum oxide nanoparticles. *J. Biomed. Matter. Res. A* **92**: 80–86.

Fahmy B, Cormier SA. 2009. Copper oxide nanoparticles induce oxidative stress and cytotoxicity in airway epithelial cells. *Toxicol. In Vitro* **23**: 1365–1371.

Fernández-Urrusuno R, Fattal E, Féger J, Couvreur P, Thérond P. 1997. Evaluation of hepatic antioxidant systems after intravenous administration of polymeric nanoparticles. *Biomaterials* **18**: 511–517.

Habig WH, Pabst MJ, Jakoby WB. 1974. Glutathione *S*-transferase. The fist enzymatic step in mercapturic acid formation. *J. Biol. Chem.* **249**: 7130–7139.

Jollow DJ, Mitchell JR, Zampaglione N, Gillete JR. 1974. Bromobenzene-induced liver necrosis. Protective role of glutathione and evidence for 3, 4-bromobenzeneoxide as the hepatotoxic metabolite. *Pharmacology* **11**: 151–169.

Kortenkamp A, Oetken G, Beyersmann D. 1990. The DNA cleavage induced by a chromium (V) complex and by chromate and glutathione is mediated by activated oxygen species. *Mutat. Res.* **232**: 155–161.

Kumar V, Bal A, Gill KD. 2009. Susceptibility of mitochondrial superoxide dismutase to aluminium induced oxidative damage. *Toxicology* **255**: 117–123.

Li JJ, Hartono D, Ong CN, Bay BH, Yung LY. 2010a. Autophagy and oxidative stress associated with gold nanoparticles. *Biomaterials* **31**: 5996–6003.

Li ZH, Li P, Randak T. 2010b. Effect of a human pharmaceutical carbamazepine on antioxidant responses in brain of a model teleost in vitro: an efficient approach to biomonitoring. *J. Appl. Toxicol.* **30**: 644–648.

Liu S, Xu L, Zhang T, Ren G, Yang Z. 2010. Oxidative stress and apoptosis induced by nanosized titanium dioxide in PC12 cells. *Toxicology* **267**: 172–177.

Lowry OH, Rosebrough NJ, Farr AL, Randall RJ. 1951. Protein measurement with the Folin-phenol reagent. *J. Biol. Chem.* **193**: 265–275.

Ma L, Liu J, Li N, Wang J, Duan Y, Yan J, Liu H, Wang H, Hong F. 2010. Oxidative stress in the brain of mice caused by translocated nanoparticulate TiO_2 delivered to the abdominal cavity. *Biomaterials* **31**: 99–105.

Mahieu S, Contini Mdel C, González M, Millen N. 2009. Melatonin reduces oxidative damage induced by aluminium in rat kidney. *Toxicol. Lett.* **190**: 9–15.

Marklund S, Marklund G. 1974. Involvement of superoxide anion radical in the autoxidation of pyrogallol and a convenient assay for superoxide dismutase. *Eur. J. Biochem.* **47**: 469–474.

Monteiro-Riviere NA, Oldenburg SJ, Inman AO. 2010. Interactions of aluminum nanoparticles with human epidermal keratinocytes. *J. Appl. Toxicol.* **30**: 276–285.

Murdock RC, Braydich-Stolle L, Schrand AM, Schlager JJ, Hussain SM. 2008. Characterization of nanomaterial dispersion in solution prior to *in vitro* exposure using dynamic light scattering technique. *Toxicol. Sci.* **101**: 239–253.

Nel A, Xia T, Madler L, Li N. 2006. Toxic potential of materials at the nanolevel. *Science* **311**: 622–627.

Oberdörster G, Maynard A, Donaldson K, Castranova V, Fitzpatrick J, Ausman K, Carter J, Karn B, Kreyling W, Lai D, Olin S, Monteiro-Riviere N, Warheit D, Yang H. 2005. Principles for characterizing the potential human health effects from exposure to nanomaterials: elements of a screening strategy. *Part. Fibre Toxicol.* **6**: 2–8.

OECD. 2001. Guideline for the Testing of Chemicals: Acute Oral Toxicity – Fixed Dose Procedure. Guideline 420. Organization for Economic Cooperation and Development: Paris.

Oesterling E, Chopra N, Gavalas V, Arzuaga X, Lim EJ, Sultana R, Butterfield DA, Bachas L, Hennig B. 2008. Alumina nanoparticles induce expression of endothelial cell adhesion molecules. *Toxicol. Lett.* **178**: 160–166.

Paglia DE, Valentine WN. 1967. Studies on qualitative and quantitative characterization of erythrocytes glutathione peroxidase. *J. Lab. Clin. Med.* **70**: 158–169.

Patlolla A, McGinnis B, Tchounwou P. 2011. Biochemical and histopathological evaluation of functionalized single-walled carbon nanotubes in Swiss–Webster mice. *J. Appl. Toxicol.* **31**: 75–83.

Powers SK, Jackson MJ. 2008. Exercise-induced oxidative stress: cellular mechanisms and impact on muscle force production. *Physiol. Rev.* **88**: 1243–1276.

Sadiq IM, Chowdhury B, Chandrasekaran N, Mukherjee A. 2009. Antimicrobial sensitivity of Escherichia coli to alumina nanoparticles. *Nanomedicine* **5**: 282–286.

Sun Z, Wang W, Wang R, Duan J, Hu Y, Ma J, Zhou J, Xie S, Lu X, Zhu Z, Chen S, Zhao Y, Xu H, Wang C, Yang X-D. 2010. Aluminum nanoparticles enhance anticancer immune response induced by tumor cell vaccine. *Cancer Nano.* **1**: 63–69.

Tyner KM, Schiffman SR, Giannelis EP. 2004. Nanobiohybrids as delivery vehicles for camptothecin. *J. Con. Re.* **95**: 501–514.

Wagner AJ, Bleckmann CA, Murdock RC, Schrand AM, Schlager JJ, Hussain SM. 2007. Cellular interaction of different forms of aluminum nanoparticles in rat alveolar macrophages. *J. Phys. Chem. B* **111**: 7353–7359.

Wang B, Feng WY, Zhu MT, Wang Y, Wang M, Gu Y, Ouyang H, Wang H, Li M, Zhao Y, Chai Z, Wang H. 2009. Neurotoxicity of low-dose repeatedly intranasal instillation of nano- and submicron-sized ferric oxide particles in mice. *J. Nanopart. Res.* **11**: 41–53.

Wang J, Chen C, Li B, Yu H, Zhao Y, Sun J, Li Y, Xing G, Yuan H, Tang J, Chen Z, Meng H, Gao Y, Ye C, Chai Z, Zhu C, Ma B, Fang X, Wan L. 2006. Antioxidative function and biodistribution of $[Gd@C82(OH)22]_n$ nanoparticles in tumor-bearing mice. *Biochem. Pharmacol.* **71**: 872–881.

Wills ED. 1969. Lipid peroxide formation in microsomes. Relation of hydroxylation to lipid peroxide formation. *Biochem. J.* **113**: 333–341.

Yang H, Liu C, Yang D, Zhang H, Xi Z. 2009. Comparative study of cytotoxicity, oxidative stress and genotoxicity induced by four typical nanomaterials: the role of particle size, shape and composition. *J. Appl. Toxicol.* **29**: 69–78.

Zhu MT, Feng WY, Wang B, Wang TC, Gu YQ, Wang M, Wang Y, Ouyang H, Zhao YL, Chai ZF. 2008. Comparative study of pulmonary responses to nano- and submicron-sized ferric oxide in rats. *Toxicology* **247**: 102–111.